RESEARCH ARTICLE

Editorial Process: Submission:07/08/2025 Acceptance:02/01/2026 Published:02/06/2026

Tumor-Intrinsic *PD-1* Regulatory Network Drives Lapatinib Resistance in *HER2*$^+$ Breast Cancer: An Integrative Bioinformatics Analysis

Ahmed S. Alhallaq*, Nadeen S. Sultan

Abstract

Background: Lapatinib resistance evolution in HER2+ breast cancer is still a crucial therapeutic hurdle, with immune microenvironmental reprogramming playing a minimally explored role. Beyond its canonical expression on T cells, programmed cell death protein 1 (*PD-1/PDCD1*) is intrinsically induced in resistant breast tumors. Through the binding of tumor-intrinsic PD-1 to PD-L1 on adjacent tumor or stromal cells, inhibitory signals are generated, establishing an immunosuppressive microenvironment. **Methods:** This exploratory study investigated the tumor-intrinsic (*PD-1)*-lapatinib resistance (PLR) regulatory network driving lapatinib resistance in *HER2*$^+$/ER–/PR– breast cancer using an integrative bioinformatics analysis. The GSE38376 dataset and *PDCD1* co-expressed genes were utilized to construct the protein-protein interaction (PPI) of the PLR regulatory network. Gene expression patters were visualized using a complex heatmap. Gene ontology, KEGG functional enrichment, gene-metabolite interaction network, immune cell infiltration, comparative gene expression profiling, correlation analysis of *PDCD1-hub* genes, survival analysis, and genetic alterations analysis were performed on the PLR regulatory network to elucidate the mechanisms of lapatinib resistance. **Results:** Pathways and gene-metabolite analyses showed that the PLR regulatory network genes were enriched in immune regulation pathways and lipid metabolic reprogramming. The top 10 PLR-hub genes were identified. Expression profiling in lapatinib-resistant cells revealed the upregulation of *PDCD1, B2M,* and *ITGB2,* while other genes, particularly those involved in interferon response and antigen presentation, were downregulated. Immune infiltration analysis indicated exhausted T cells and an immunosuppressive microenvironment. Comparative gene expression and survival analyses of PLR-hub genes implicated the PLR regulatory network in lapatinib resistance. Genetic alterations were infrequent, suggesting that regulation may occur epigenetically or transcriptionally. **Conclusion:** The findings revealed that the PLR regulatory network is associated with *HER2*$^+$/ER–/PR– lapatinib resistance through multiple mechanisms, including interferon signaling silencing, T cell exhaustion, and the fostering of an immunosuppressive niche. These insights pave the way for interventions aimed at overcoming lapatinib resistance in HER2$^+$ breast cancer.

Keywords: Tumor-intrinsic PD-1- cancer cell-intrinsic PD-1- lapatinib resistance- HER2+ breast cancer

Asian Pac J Cancer Prev, **27 (2)**, 613-627

Introduction

Human epidermal growth factor receptor 2 (*HER2*, ErbB2) amplification promotes aggressive breast cancer phenotypes via fueling downstream oncogenic signaling. *HER2* is targeted by receptor tyrosine kinase inhibitors such as lapatinib, a dual EGFR/*HER2* suppressor that hinders receptor autophosphorylation and downstream signaling. Although lapatinib initially shows efficacy in *HER2*$^+$ breast cancer, resistance frequently emerges through oncogenic mechanisms, including *HER2* bypass via PI3K/Akt/mTOR activation and epithelial-mesenchymal transition (EMT). Emerging evidence also implicates tumor microenvironment (TME) reprogramming and immune-evasion mechanisms as critical drivers of therapeutic escape [1]. Breast tumors can modulate lapatinib response by developing rigid extracellular matrices via YAP/TAZ signaling, disrupting immune cell infiltration [2].

Programmed cell death protein 1 (*PDCD1*, *PD-1*, CD279) is an inhibitory immune checkpoint expressed on activated T cells that, upon binding with its ligands *PD-L1* or *PD-L2*, stimulates SHP2 phosphatase to dephosphorylate T cell receptor (TCR) signaling molecules and enforce T cell exhaustion, a state of functional impairment characterized by lower cytokine synthesis and proliferative potency [3]. The *PD-1* pathway is co-opted to evade anti-tumor immunity by breast tumors. Although classically expressed on T cells, *PD-1* is intrinsically upregulated in resistant breast cancer

*Laboratory Medicine Department, Faculty of Applied Medical Sciences, Al-Azhar University-Gaza, Gaza Strip, Palestine. *For Correspondence: ahmdhallag@gmail.com*

cells, where it delivers SHP2-dependent inhibitory signals that dampen TCR signaling and tumor cell apoptosis pathways. Cancer cell-intrinsic *PD-1* remodels the TME, suppressing anti-tumor immunity, and drives malignant progression. By the binding of cancer cell-intrinsic *PD-1* to *PD-L1* on adjacent tumor or stromal cells, inhibitory signals are generated that reduce CD8+ T cells, effector T cell infiltration, and establish an immunosuppressive microenvironment [4]. Tumor-intrinsic *PD-1* is a critical driver of tumor therapy resistance through direct, immune-independent mechanisms that simultaneously shape an immunosuppressive TME. In cancers such as melanoma, hepatocellular carcinoma, and glioblastoma, cancer cell-intrinsic *PD-1* activation promotes tumor growth and self-renewal by directly stimulating oncogenic pathways, including mTOR and NF-κB. Conversely, in non-small cell lung and colon cancers, tumor-intrinsic *PD-1* unexpectedly functions as a tumor suppressor, so its blockade can inadvertently accelerate disease. This dual role, dictated by tumor type and upstream drivers like p53, allows tumor-intrinsic *PD-1* to fuel malignancy directly and contribute to a cold TME, creating a formidable barrier to the efficacy of immunotherapy [9].

Regulatory mechanisms of *PD-1*/PD L1 in cancers include transcriptional regulation by interferon signaling, epigenetic modifications, canonical NF-κB signaling, and microenvironmental cytokines such as IFNγ and TNFα [5, 6]. Evidence highlight that *HER2* signaling intersecting with immune checkpoints affects TME and drug sensitivity. For instance, trastuzumab, another *HER2*-targeting antibody, triggers *PD-L1* via NF κB stimulation, attenuating drug efficacy and promoting an immune suppression signature [2, 5, 7, 8]. Lapatinib modulates cytokine release and may prime tumors for checkpoint blockade, yet the molecular networks linking tumor-intrinsic *PD-1* regulation to lapatinib resistance remain undefined [9, 10].

This study aims to investigate the tumor-intrinsic *PDCD1*-lapatinib resistance (PLR) regulatory network driving lapatinib resistance in *HER2*+ breast cancer via integrative bioinformatic and transcriptomic analyses.

Materials and Methods

Lapatinib structure and lapatinib-protein interaction network construction

The chemical structure and formula of lapatinib were obtained from the Drug Bank database (DrugBank ID: DB01259; https://go.drugbank.com/drugs/DB01259). The lapatinib-protein interaction network was retrieved from the STITCH database (version 5.0; http://stitch.embl.de/) by querying the compound identifier "lapatinib" and organism identifier "Homo Sapiens". The lapatinib-protein interactions were filtered to include only those with a high confidence score ≥ 0.7.

Data mining and processing

Tumor-intrinsic *PDCD1* co-expressed genes were retrieved from the TCGA dataset from cBioportal (https://www.cbioportal.org/), a cancer genomics database, using the keywords "*PDCD1*" and "breast cancer". Firehose legacy and Cell 2015 datasets were merged, then the dplyr package in R filtered the data based on a p-value less than 0.05 and Spearman's correlation values ≥0.4 or ≤-0.4. Regulatory genes implicated in *HER2*$^+$/ER–/PR– breast cancer resistance to lapatinib were obtained from the Gene Expression Omnibus (GEO; https://www.ncbi.nlm.nih.gov/geo/) database, a resource containing high-throughput gene expression data, microarray, RNA-Seq, and other forms of genomics data. The search strategy targeted datasets related to lapatinib-resistant *HER2*$^+$/ER–/PR– breast cancer based on the terms "lapatinib-resistant" and "lapatinib-sensitive" in the search query using the advanced search. For an exploratory bioinformatics study, the inclusion criteria were human *HER2*$^+$/ER–/PR– breast cancer with at least three samples per group, and the presence of 4 groups: lapatinib-resistant control (RC), lapatinib-resistant treated (RT), lapatinib-sensitive control (SC), and lapatinib-sensitive treated (ST) groups, to ensure minimal statistical validity. The exclusion criteria were non-human studies and datasets with a small sample size. One dataset was selected, GSE38376, which was generated using the GPL6947 Illumina HumanHT-12 V3.0 expression beadchip platform. The GSE38376 dataset comprises 18 samples of *HER2*$^+$/ER–/PR– SKBR3 and SKBR3-R breast cancer cells, 3 RC, 6 RT (3 samples treated with 0.1 μM and 3 samples treated with 1 μM), 3 SC, and 6 ST (3 samples treated with 0.1 μM and 3 samples treated with 1 μM) [11]. The GEO2R tool was used to analyze differentially expressed genes (DEGs) of the GSE38376 dataset based on the R programming packages, including limma, a well-known R package for microarray analysis, which performs statistical analysis, and the GEOquery and umap packages. The GEO2R tool provides normalized data, log2-fold change determination, and adjusted p-values using the Benjamini-Hochberg method (FDR, False discovery rate). The generated gene list was downloaded, and the dplyr package filtered the significant genes based on a log2-fold change >1 (2× change) and an adjusted p-value less than 0.05. Differential expression analysis was performed using the limma package. Pairwise contrasts were generated cyclically (For instance, RC/RT, RT/SC, SC/ST, ST/RC), where the numerator is the first group and the denominator is the second. Genes were ranked by the moderated F-statistic, which accounts for variance moderation across genes, allowing robust identification of those with the strongest differential expression. The intersection of *PDCD1* co-expression data from cBioportal and lapatinib resistance data from GSE38376 was retrieved using Venny 2.1.0 (https://bioinfogp.cnb.csic.es/tools/venny/), and data were considered overlapping genes implicated in the *PDCD1*-lapatinib resistance (PLR) regulatory network. Then, the PLR genes with strong Spearman's correlation values ≥0.6 or ≤-0.6 were identified by utilizing the dplyr package.

Microarray data processing and representation of PLR-DEGs

The expression matrix file for the GSE38376 dataset was processed, checked for quality control, and normalized using R packages. A log2-fold change >1, FDR < 0.05, and adjusted p-value less than 0.05 were

considered the threshold values for PLR-DEGs. The annotation of probe identifiers with gene symbols was performed using the GEOquery package, which depends on the GPL6947 Illumina HumanHT-12 V3.0 expression beadchip platform. Genes mapped to multiple probes were aggregated by calculating their mean values. In addition, the heatmap was constructed using the ComplexHeatmap R package to showcase the significant PLR-DEGs, and gene expression data were represented as z-scores.

Gene ontology and KEGG pathway enrichment analysis

Gene ontology enrichment of PLR genes was performed using an over-representative analysis (ORA) and a genome protein-coding reference set on WebGestalt (http://www.webgestalt.org/process.php). In this test, the biological process, cellular component, and molecular function were analyzed, and the results were visualized as bar plots and interpreted accordingly. The selection criteria for PLR genes submitted to the server for analysis were ORA query, FDR < 0.05, and the Benjamini-Hochberg method for multiple test adjustment. Gene-Terms network is processed using the dplyr and tidyr packages and constructed via the ggraph, tidygraph, and igraph packages in R. The network illustrates common genes and central biological processes among the significantly enriched gene ontology terms. In addition, the Term-Gene association heatmap is processed using the dplyr and tidyr packages and constructed via the ggplot2 package in R. This plot exhibits core genes involved in several enriched biological processes, demonstrating they may be key regulators or biomarkers in lapatinib-resistant breast cancer. Data with p-value < 0.05 are selected and presented for the network and heatmap.

PLR genes were analyzed for the Kyoto Encyclopedia of genes and genomes (KEGG) pathway using Database for Annotation, Visualization, and Integrated Discovery (DAVID version 6.8; https://david.ncifcrf.gov/tools.Jsp), a set of functional annotation tools. PLR genes were submitted to the server for analysis as a query in DAVID with Homo Sapiens and FDR < 0.05 as selection criteria. A scatter plots (bubble plot) were created in R using the ggplot2 package to represent significantly enriched KEGG pathways and clusters, with a p-value < 0.05. Modified Fisher's exact test was used to analyze data, and Benjamini-Hochberg FDR was applied for multiple testing correction.

Construction of protein-protein interaction network and selection of hub genes

The protein-protein interaction (PPI) network was analyzed and constructed using Search Tool for the Retrieval of Interacting Genes/Proteins (STRING version 12.0; https://string-db.org/), a resource that predicts protein-protein interactions. PLR genes were uploaded based on the settings selection of "Homo sapiens" model, medium FDR stringency < 0.05, and 0.4 confidence for the interaction between the targets. The network nodes exhibited proteins, and edges reflected the PLR protein-protein interactions. Using the CytoHubba plugin of Cytoscape, hub genes were identified based on degree ranking, and the top 10 genes with the highest scores were selected for further analysis.

Construction of gene-metabolite interaction network

The gene-metabolite interaction network was analyzed and constructed using the MetaboAnalyst tool (https://www.metaboanalyst.ca/), a comprehensive metabolomics data analysis platform presenting functional and integrative analysis tools. The chemical and human gene associations are extracted from STITCH, and only high-confidence interactions are obtained.

Correlation between PLR-hub gene expression and infiltration of immune cells

The association between *PLR-hub* gene expression and immune cell infiltration was analyzed using Tumor Immune Estimation Resource 2.0 (TIMER2.0; http://timer.cistrome.org/), a bioinformatics tool designed to analyze and visualize tumor-infiltrating immune cells using deconvolution algorithms across various cancer types, including *HER2*$^+$ breast cancer. Spearman's correlation values were selected for BRCA-*HER2*$^+$ samples. The Wilcoxon signed-rank test is used to analyze data. The corrplot package in R was utilized to visualize the correlation between *PLR-hub* gene expression and infiltration of immune cells in *HER2*$^+$ breast tumors, and the significant associations are labeled with stars. On the other hand, the immune cell composition analysis in the lapatinib-resistant GSE38376 dataset was conducted using CIBERSORTx (https://cibersortx.stanford.edu/), a deconvolution algorithm-based computational tool designed to quantify the immune cell composition based on normalized gene expression profiles [12]. The absolute mode quantification and LM22 leukocyte signature matrix were selected to estimate cell-type-specific abundances from bulk gene expression data of the GSE38376 matrix file. The absolute cell fractions were imputed, and B-mode batch correction, quantile normalization, and 1,000 permutations were chosen for the analysis, mitigating technical variability, standardizing distributions across samples, and reducing statistical bias. The findings of absolute quantification were normalized and visualized via a dual-encoded bubble plot using the R ggplot2 package.

Comparative gene expression of PLR-hub genes in breast cancer samples

Gene expression analysis of the *PLR-hub* genes in normal and tumor breast tissues was conducted using Gene Expression Profiling Interactive Analysis (*GEPIA*; http://*GEPIA*.cancer-pku.cn/index.html), a bioinformatics web-based tool designed for comprehensive gene expression analysis. The BRCA datasets of the TCGA were utilized to compare hub gene expression between normal and tumor breast tissues, and Student's t-test was applied for statistical analysis. Expression levels of *PLR-hub* genes in normal, tumor, and metastatic breast cancer tissues were assessed using TNMPlot (https://tnmplot.com/analysis/), with statistical comparisons across the three groups performed using the Kruskal–Wallis test. The University of ALabama at Birmingham CANcer data analysis Portal (UALCAN; https://ualcan.path.uab.edu/), a resource designed for analyzing cancer OMICS data, was

utilized to investigate the *PLR-hub* gene expression in normal breast tissues as well as major subtypes of breast cancer, including *HER2*$^+$ breast cancer. Welch's t-test was applied to compare the normal group with the *HER2*$^+$ group, as the two groups have unequal variances and sample sizes. *PLR-hub* gene expression analysis in *HER2*$^+$ and *HER2*– breast cancer samples was conducted using the Breast Cancer Gene-Expression Miner v5.2 portal (bc-GenExMiner v5.2; https://bcgenex.ico.unicancer.fr/BC-GEM/GEM-Requete.php?mode=8), and Welch's t-test was used for statistical comparison. Moreover, UALCAN (https://ualcan.path.uab.edu/) was utilized to investigate the *PLR-hub* gene expression based on *TP53* mutation status, providing a deeper insight into the role of *PLR-hub* genes in *TP53*-mutant and non-mutant breast cancer. *TP53* mutation status was obtained from TCGA whole-exome sequencing data, and the samples with or without *TP53* mutation were matched with RNA-seq data. Welch's t-test was applied to compare the three groups, as all groups have unequal variances and sample sizes.

Correlation between the gene expression of PDCD1 and PLR-hub genes

The correlation between *PDCD1* and *PLR-hub* genes in *BRCA-HER2*$^+$ samples was analyzed using TCGA breast cancer datasets in *GEPIA* (http://*GEPIA*.cancer-pku.cn/) and TIMER2.0 (http://timer.cistrome.org/). Spearman's correlation and derived p-value from the strength of the association were exploited to estimate the level of correlation in both *GEPIA* and TIMER 2.0 platforms. The ggplot2 package in R was used to generate scatter plots representing correlations.

Survival analysis

PDCD1 and *PLR-hub* gene prognostic values were estimated by Kaplan-Meier Plotter (KMPlotter; https://kmplot.com/analysis/), a tool for survival analysis based on databases such as GEO, EGA, TCGA, Metabric, Impact, and PubMed repositories. The selection criteria were *HER2*$^+$/ER–/PR– breast cancer, and the observations are exhibited as hazard ratio (HR) and relapse-free survival (RFS). The significance level is calculated via the Log-Rank Test (Mantel-Cox test). The ggplot2 package in R generated a forest-style horizontal dot plot.

Genetic alteration analysis of PDCD1 and PLR-hub genes

PDCD1 and *PLR-hub* gene genetic alterations were investigated using cBioportal (https://www.cbioportal.org/), depending on the PanCancer Atlas study for oncoprint, co-occurrence tendency, and mutual exclusivity analysis. TCGA breast invasive carcinoma and samples with mutations and Copy Number Alteration (CNA) were selected as criteria. For co-occurrence tendency, the two-sided Fisher Exact Test was applied to evaluate the significance level, and the Benjamini-Hochberg method (FDR correction procedure) was utilized for adjustment. Genetic alterations of *PLR-hub* genes were represented as a log-scale box and whisker plot.

Statistical analysis

Data analyses and visualizations were conducted using the R programming language version 4.3.3. A p-value threshold of less than 0.05 was considered statistically significant.

Results

Lapatinib-protein interaction network

The lapatinib-protein interaction network shows strong interactions with the ErbB receptor family, including ErbB2 (*HER2*$^+$) and EGFR (both with a score of 0.999), followed by ERBB3 (0.976) and ERBB4 (0.967), underscoring its role as a dual *HER2*$^+$/EGFR tyrosine kinase inhibitor (Figure 1A and 1B). Lapatinib is also associated with signaling molecules such as AKT1, a part of PI3K/AKT signaling. Furthermore, VEGFA, ABCC10, MCL1, ESR1, and the tumor suppressor *TP53* may also be affected via lapatinib. The network also demonstrated a broad spectrum of protein-protein interactions, which may influence therapeutic response and resistance.

Data mining and identification of the PDCD1-lapatinib resistance regulatory network

Following the filtration of genes based on p-value less than 0.05 and Spearman's correlation values ≥0.4 or ≤-0.4, the Firehose legacy and Cell 2015 TCGA Breast cancer datasets from cBioportal were merged. 1083 *PDCD1* co-expressed genes, 1071 with positive and 12 with negative correlations, were obtained. For lapatinib-resistant *HER2*$^+$/ER–/PR– breast cancer, the GSE38376 dataset met the criteria and was selected. The GSE38376 dataset includes 18 samples of *HER2*$^+$/ER–/PR– SKBR3 and SKBR3-R breast cancer cells, 3 RC, 6 RT, 3 SC, and 6 ST. Following the dataset analysis using GEO2R, the median expression intensities via boxplot indicated normalized comparable distribution profiles between the samples (Figure 1C). Uniform manifold approximation and projection (UMAP) plot for the 4 groups exhibited consistency and similarity in the characteristics within each group (Figure 1D). Genes were filtered based on adjusted p-value less than 0.05, and 5,694 significant genes implicated in lapatinib-resistant breast cancer were selected. The intersection between 1083 *PDCD1* co-expressed genes and 5,694 lapatinib-resistant breast cancer genes was determined using Venny 2.1.0 (Figure 1E). From the resulting 187 PLR genes, 49 PLR regulatory network genes with strong Spearman's correlation values ≥0.6 or ≤-0.6 were picked.

To build a heatmap for PLR genes based on microarray data, the GSE38376 dataset expression matrix file was checked for quality control, normalized, and screened using R packages based on the following criteria: log2-fold change >1, FDR < 0.05, and adjusted p-value less than 0.05. Then, *PDCD1* and 49 PLR gene expressions were visualized using a complex heatmap based on z-scores, showing a clear clustering between the samples of the 4 groups, thus underlining the robustness of the gene expression variations observed (Figure 1F). Of these, *PDCD1* and 49 PLR regulatory network, 12 genes were upregulated, while 38 were downregulated in the lapatinib-resistant groups (Table 1). These findings highlight the molecular differences between

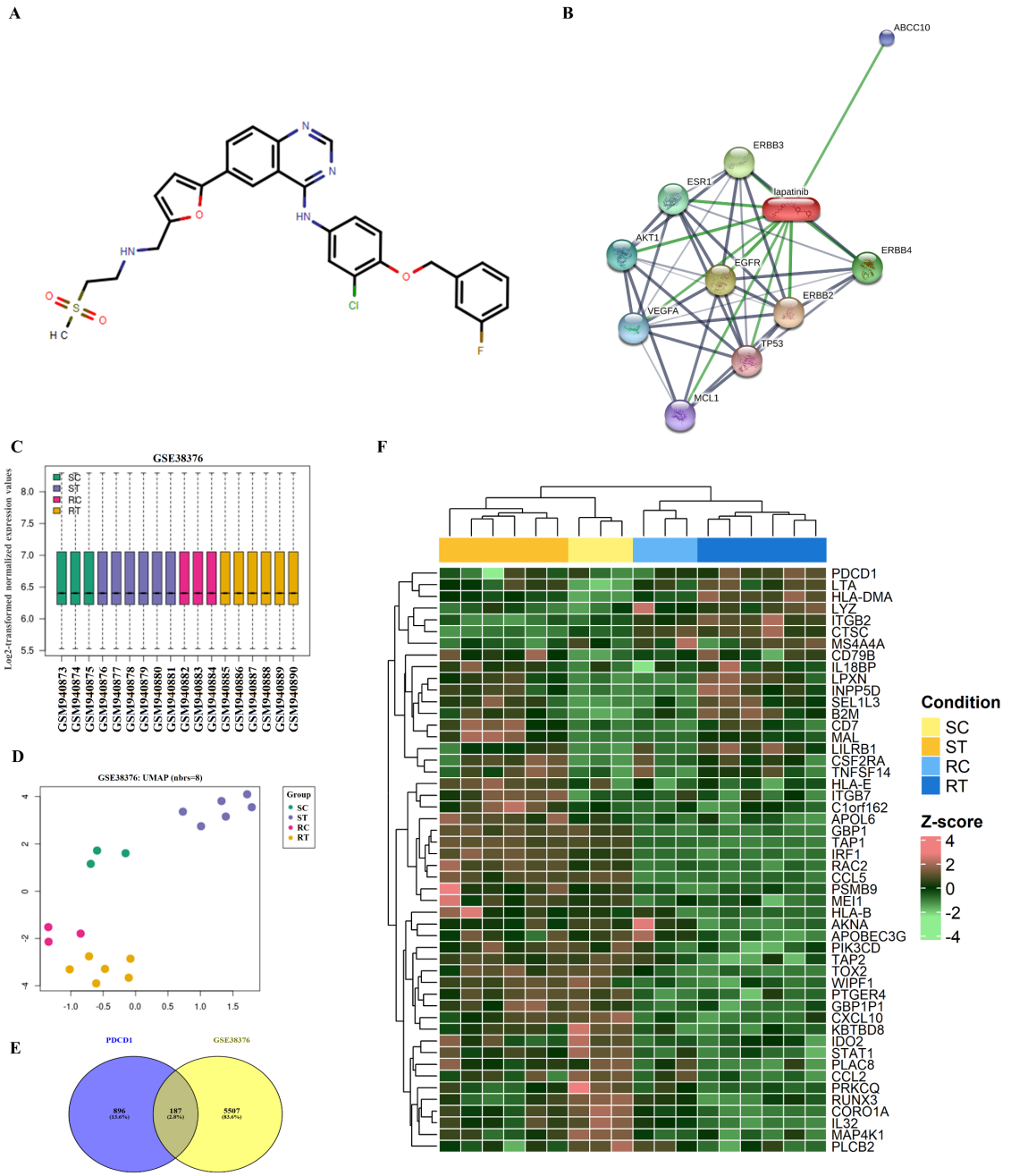

Figure 1. Lapatinib Structure and Interactions, Data Processing, and Differential Expression Analysis of SC, ST, RC, and RT Breast Cancer Groups. (A) Lapatinib structure derived from the Drug Bank. The chemical formula of lapatinib is $C_{29}H_{26}ClFN_4O_4S$. (B) Lapatinib-protein interactions network constructed using the STITCH tool. Protein-protein interactions are represented in grey, and chemical-protein interactions in green. Lapatinib directly interrupts HER2/neu and epidermal growth factor receptor (EGFR) pathways. (C) Intensity distribution boxplot of 18 samples of the GSE38376 dataset based on log2-transformed normalized expression values. Median-centered values of 18 samples indicate that the data are normalized and cross-comparable. (D) UMAP plot of 18 samples of the GSE38376 dataset. The UMAP plot exhibits that the 18 samples, SC, ST, RC, and RT, are clustered based on expression similarity. This supports the idea that resistant groups deviate from sensitive groups based on DEGs. (E) Venn diagram of lapatinib resistance DEGs and PDCD1 regulatory network, resulting in 187 genes that are considered genes involved in the PLR regulatory network. (F) Heatmap of the PDCD1 and 49 differentially expressed PLR regulatory network genes with strong Spearman's correlation values ≥0.6 or ≤-0.6 between SC, ST, RC, and RT groups.

Table 1. Upregulated and Downregulated PLR Genes in the Lapatinib-Resistant Groups

Upregulated PLR Genes	Downregulated PLR Genes
B2M, CTSC, HLA-DMA, INPP5D, ITGB2, LILRB1, LPXN, LTA, LYZ, MS4A4A, SEL1L3, PDCD1.	*AKNA, APOBEC3G, APOL6, C1orf162, CCL2, CCL5, CD7, CD79B, CORO1A, CSF2RA, CXCL10, GBP1, HLA-B, HLA-E, IL18BP, IL32, IRF1, ITGB7, KBTBD8, MAL, MAP4K1, MEI1, PIK3CD, PLAC8, PLCB2, PRKCQ, PSMB9, PTGER4, RAC2, RUNX3, STAT1, TAP1, TAP2, TNFSF14, WIPF1, GBP1P1, IDO2, TOX2.*

lapatinib-sensitive and lapatinib-resistant breast cancers. The distinct up- and downregulation of specific genes proposes intricate molecular mechanisms playing a role in the evolution of breast cancer clones resistant to lapatinib. The selected PLR regulatory network genes present a promising basis for further investigations into the mechanisms underlying breast cancer resistance to lapatinib and potential therapeutic targets.

Gene ontology and KEGG pathway enrichment analysis

Gene ontology enrichment analysis shows *PDCD1* and PLR regulatory network genes' relation to biological processes, cellular components, and molecular functions (Figure 2A). Gene Ontology enrichment analysis revealed significant immune-related biological processes, with the top 20 enriched terms dominated by adaptive immunity (GO:0002250, p = 7.34e-14), leukocyte adhesion (GO:0007159, p = 5.94e-11), and immune regulation (GO:0002683, p = 1.06e-7). These terms exhibited high enrichment ratios (up to 11.96) and stringent statistical significance (FDR < 1e-6), indicating association with immune activation and regulatory mechanisms. For example, genes including *CCL5, HLA-E, PIK3CD, IRF1,* and *STAT1* recur across several gene ontology terms, underscoring their role as central hubs in immune regulation. The network plot demonstrated dense connectivity between clusters, 81 nodes and 341 edges, and the highly connected nodes are positioned centrally (Figure 2B). For example, the network shows dense connectivity between adaptive immunity and cell adhesion clusters, sharing genes like *HLA-E, ITGB2*, and *CCL5*. The heatmap further delineated gene-term associations, revealing chemokines such as *CCL5* as multifunctional molecules in cytokine signaling and cell migration (Figure 2C). *CXCL10* and *CCL2* dominate chemotaxis-associated terms. *PDCD1* appears exclusively in adaptive immunity terms, reflecting its function as an immune checkpoint. The heatmap exhibits multifunctional genes such as *IRF1* and *STAT1* acting across interferon response and leukocyte activation. Furthermore, the heatmap emphasizes gene pleiotropy; for example, *CCL5* exists in both chemotaxis and cytokine production. The readouts illustrate a connected and regulated immune network with *PDCD1-PLR* genes, suggesting potential therapeutic targets for modulating immune responses in contexts such as *PD-1*-mediated lapatinib resistance.

KEGG pathway enrichment analysis of *PDCD1* and PLR genes revealed 27 highly enriched pathways (Fold

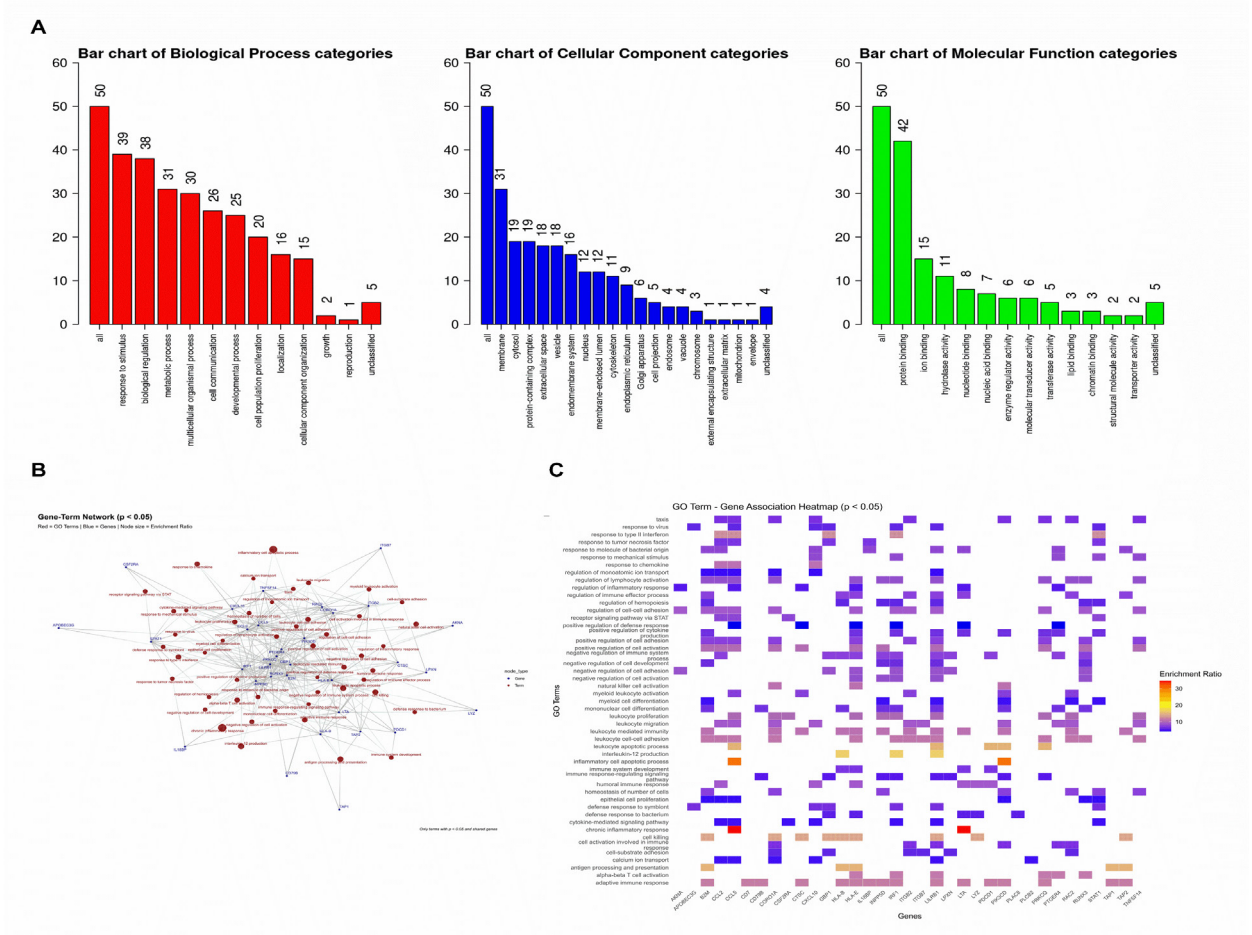

Figure 2. Gene Ontology Enrichment of PDCD1 and 49 PLR Regulatory Network in Homo Sapiens. (A) Gene ontology enrichment analysis of *PDCD1* and *49 PLR* genes with strong Spearman's correlation values ≥0.6 or ≤-0.6. This bar chart presents genes involved in biological processes, cellular components, and molecular functions. (B) Gene-Terms network for the significantly enriched gene ontology terms. This network helps to identify shared genes and core biological processes. (C) Term-gene association heatmap for the significantly enriched terms and shared genes. For the network and heatmap, the significant data with P<0.05 were selected and presented.

Enrichment (FE) ≥ 5.0) that dominate the outcomes, indicating strong biological relevance. For example, herpes simplex virus 1 infection (FE = 15.2), antigen processing (FE = 17.1), type I diabetes (FE = 20.97), Epstein-Barr virus infection (FE = 11.3), viral myocarditis (FE = 16.5), and B cell receptor signaling (FE = 12.7). These 6 pathways exceed FE 10.0. KEGG pathway enrichment analysis revealed 34 moderately enriched pathways (FE ≥ 2.0), reflecting broad stimulation of immune and viral response mechanisms. All these pathways are biologically impactful, with viral infection and immune regulation pathways showing the strongest enrichment. Significant KEGG pathway enrichment is provided with p-value, gene count, and FE (Figure 3A). KEGG pathway enrichment analysis of *PDCD1* and PLR genes generated 5 significant clusters (Figure 3B). Cluster 1 (Enrichment Score: 4.40) is associated with viral infection and immune response. The top significant key genes of *cluster 1 are HLA-DMA, HLA-B, HLA-E, STAT1, CCL5, LTA, TAP1, B2M,* and *TAP2*. Cluster 2 (Enrichment Score: 1.97) is associated with B cell and Fc receptor signaling. The top significant key genes of *cluster 2 are INPP5D, RAC2, CD79B*, and *PIK3CD*. *Cluster 3* (Enrichment Score: 1.70) is associated with cytokine/chemokine signaling and inflammation. The top significant key genes of cluster 3 are *CCL5, CCL2, STAT1, IRF1, PLCB2, CXCL10*, and *PIK3CD*. Cluster 4 (Enrichment Score: 1.34) is associated with viral carcinogenesis and hormone signaling. The top significant key genes of *cluster 4 are STAT1, IRF1, HLA-B, HLA-E,* and *PIK3CD*. Cluster 5 (Enrichment Score: 0.88) is associated with metabolic signaling. The top significant key genes of cluster 5 are *INPP5D, PIK3CD, IDO2*, and *PLCB2*. These clusters could be involved in lapatinib resistance via several mechanisms, including immune evasion, oncogenic signaling activation, recruiting immunosuppressive cells via cytokine storm, and metabolic reprogramming.

Construction of protein-protein interaction network and selection of hub genes

The PPI network of PLR genes is constructed using the STRING database, and the criteria include medium FDR stringency < 0.05 and 0.4 confidence for the target interaction. The network nodes represent the proteins, while the edges reflect the PLR protein-protein interactions. The PLR regulatory network is densely connected, and its characteristics are 48 nodes, 129 edges, 5.38 average node degree, 0.517 average local clustering coefficient, 22 expected number of edges, and < 1.0e-16 PPI enrichment p-value, implying a strong interconnectedness among the encoded proteins (Figure 4A). The interaction network generated in STRING incorporated multiple evidence types, including text-mining, experiments, databases, co-expression, neighborhood, gene fusion, and co-occurrence. *GBP1P1* is not involved in the PPI-PLR network due to its classification as a pseudogene, specifically a pseudogene of the *GBP1* gene. However, the *GBP1P1* pseudogene is non-functional and, like other pseudogenes, it might still have regulatory roles, such as acting as a competing endogenous RNA or being transcribed into non-coding RNA, but not a protein-coding role as it lacks a valid open reading frame for translation into a functional protein. The *PLR-hub* gene selection is conducted using the CytoHubba plugin of Cytoscape, and the findings contain the top 10 *PLR-hub* regulatory network genes with the highest degree scores (Table 2).

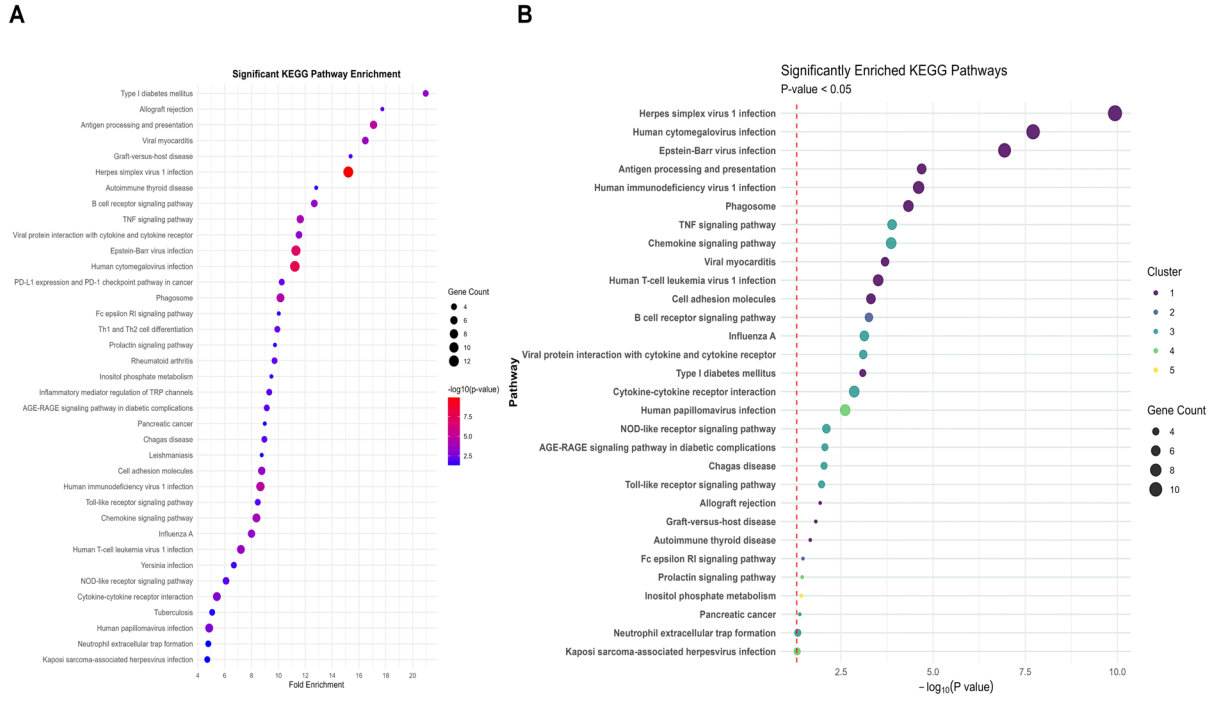

Figure 3. KEGG Pathway Enrichment Analysis of PDCD1 and 49 PLR Regulatory Network in Homo Sapiens. (A) The significantly enriched KEGG pathways. (B) The significantly enriched KEGG Functional Clusters. Data with a p-value < 0.05 were included and considered significant for KEGG pathways and clusters. Modified Fisher's exact test was used to analyze data, and Benjamini-Hochberg FDR was applied for multiple testing correction.

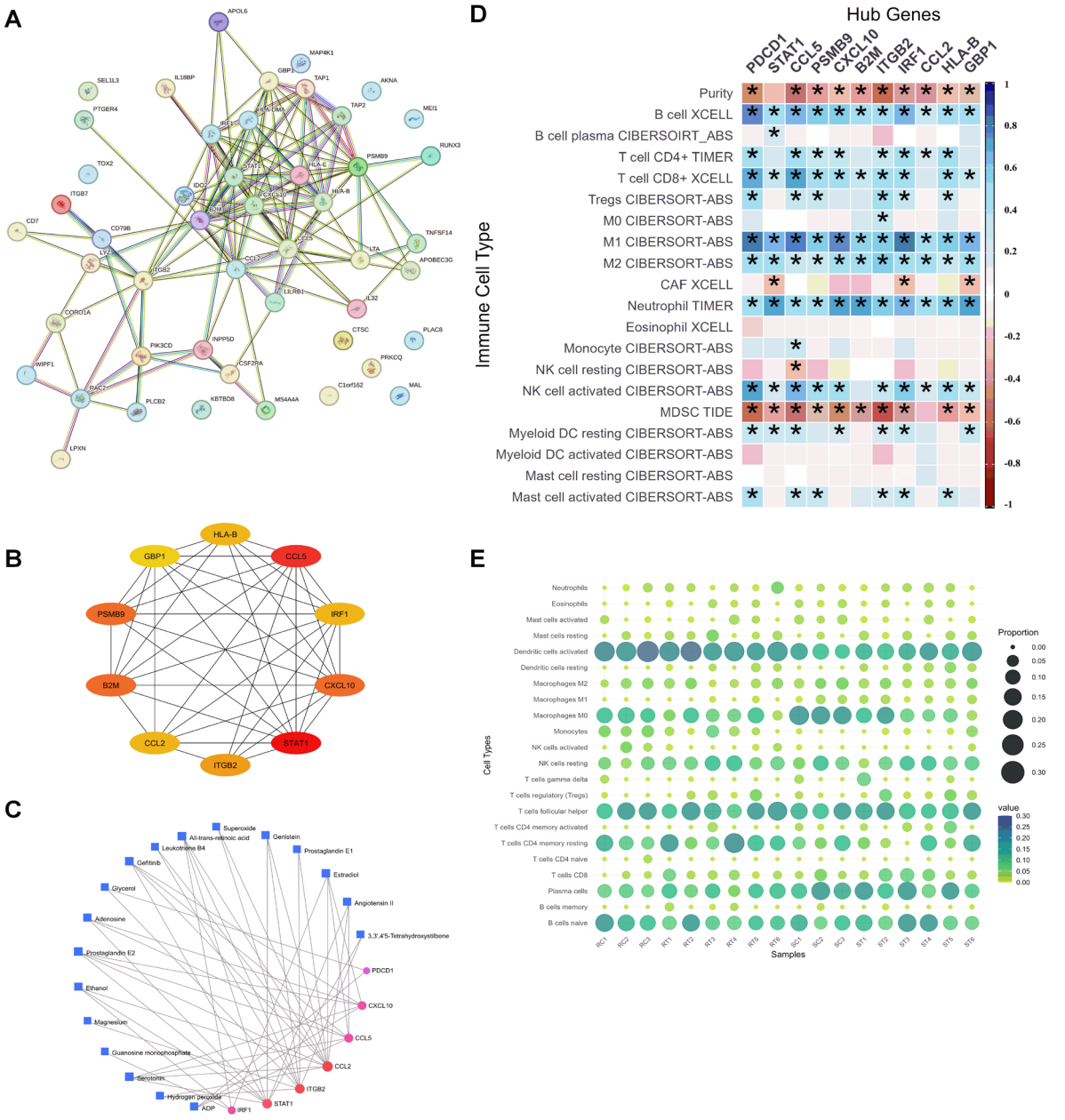

Figure 4. PPI Network and top *10 hub* Genes of PLR and Their Correlation with Metabolites and Immune cell Infiltration in HER2+ Breast Cancer. (A) PPI network of the PLR genes from the STRING database. PLR genes are highly associated, indicating their involvement in lapatinib-resistant breast cancer. (B) Top 10 PLR-hub genes depending on degree score. (C) Gene-metabolite interaction network. This analysis was performed using the MetaboAnalyst tool. (D) Correlation analysis of gene expression of *PDCD1* and the top *10 PLR-hub* genes with immune cell infiltration in HER2+ breast cancer. Immune deconvolution analysis was performed using TIMER 2.0, and the corrplot package in R visualizes the correlation. (E) Immune deconvolution analysis of the differentially infiltrated immune cells in the GSE38376 lapatinib-resistant dataset. Spearman's correlation and Wilcoxon signed-rank tests were utilized to analyze data; *P<0.05.

The *PLR-hub* regulatory network genes are *STAT1, CCL5, PSMB9, CXCL10, B2M, ITGB2, IRF1, CCL2, HLA-B,* and *GBP1* (Figure 4B). The dense interconnectivity among the 10 *PLR-hub* regulatory network proteins suggests they likely function in a coordinated rather than independent pattern. This potential shared or cooperative role supported the decision to retain all the genes for the next analyses.

Construction of gene-metabolite interaction network

The gene-metabolite interaction network of PLR genes is constructed using the MetaboAnalyst tool. The outputs show that *CCL2, ITGB2, STAT1, CCL5, CXCL10, IRF1*, and *PDCD1* genes are associated with many metabolites including, gefitinib, glycerol, leukotriene B4, all-trans-retinoic acid, superoxide, adenosine, prostaglandin E2, genistein, prostaglandin E1, estradiol, angiotensin II, 3,3',4'5-tetrahydroxystilbene, ethanol, magnesium, guanosine monophosphate, serotonin, hydrogen peroxide, and ADP (Figure 4C). The PLR gene-metabolite interaction network is highly connected, and its characteristics are 25 nodes, 49 edges, and 7 seeds.

Table 2. The Top 10 Tumor-Intrinsic PLR Regulatory Network Genes Ranked Using the Degree Method

No	PLR network proteins	Degree score
1	Signal Transducer and Activator of Transcription 1 (STAT1)	18
2	C-C Motif Chemokine Ligand 5 (CCL5)	16
3	Proteasome Subunit Beta 9 (PSMB9)	15
4	C-X-C Motif Chemokine Ligand 10 (CXCL10)	15
5	Beta-2-Microglobulin (B2M)	15
6	Integrin Subunit Beta 2 (ITGB2)	14
7	Interferon Regulatory Factor 1 (IRF1)	13
8	C-C Motif Chemokine Ligand 2 (CCL2)	13
9	Major Histocompatibility Complex, Class I, B (HLA-B)	13
10	Guanylate Binding Protein 1 (GBP1)	11

These compounds are involved in lipid metabolism and signaling, energy metabolism, redox balance, nucleotide metabolism, amino acid metabolism, polyphenols, and pharmacological agents.

Immune dysfunction characterizes the lapatinib-resistant HER2⁺ TME

PLR-hub regulatory network genes are negatively associated with *HER2*⁺ breast tumor purity, implying that higher expression of these genes is correlated with lower tumor purity, and thus, more immune cell infiltration. Most *PLR-hub* regulatory network genes are positively associated with infiltration of B cells, CD4+, CD8+, Tregs, NK-activated cells, and mast-activated cells. On the other hand, M1 and M2 macrophages are positively associated with all *PLR-hub* regulatory network genes; thus, they are infiltrated into the TME. In addition, all *PLR-hub* genes are positively correlated with neutrophil infiltration. A weak positive correlation between the *PLR-hub* regulatory network and the myeloid dendritic resting cells is observed. On the other hand, upregulated *PLR-hub* genes are negatively correlated with the infiltration of myeloid-derived suppressor cells (MDSCs). Cancer-associated fibroblasts (CAFs) negatively correlate with high *STAT1*, *IRF1*, and *GBP1* expression in *HER2*⁺ breast tumors. Figure 4D shows the correlation between *PLR-hub* regulatory network genes and immune cell infiltration. The gene expression of *PDCD1-PLR-hub* genes in the lapatinib-resistant group shows that *PDCD1*, ITGB2, and B2M genes are upregulated compared to the rest of the PLR genes (*STAT1, CCL5, PSMB9, CXCL10, IRF1, CCL2, HLA-B,* and *GBP1*), which are downregulated. Thus, the immune signature and infiltration differ in the lapatinib-resistant conditions. Therefore, immune deconvolution analysis of the differentially infiltrated immune cells was performed on the GSE38376 lapatinib-resistant dataset (Figure 4E). The results show that naïve B cells, naïve M0 macrophages, activated dendritic cells, and T follicular helper cells are elevated in lapatinib-sensitive and -resistant samples. M2 macrophages in resistant samples are more abundant than M1. Plasma cells are increased in lapatinib-sensitive and lapatinib-resistant samples, but with a higher increase in the sensitive group. The resting NK cells and CD4+ memory cells dominate over their active, inhibited forms. CD8+ T cells, monocytes, Tregs, and neutrophils are minimally or moderately infiltrated in resistant samples. This pattern predicts a *HER2*⁺ lapatinib-resistant breast cancer TME characterized by T cell exhaustion and reduced overall anti-tumor immune cell infiltration, and thus an immunosuppressive microenvironment.

Gene expression of PLR-hub genes in breast cancer samples

The expression pattern of *PDCD1-PLR* genes in normal breast tissues and tumor breast tissues was explored via *GEPIA*. Most *PDCD1-PLR* genes are upregulated in tumor breast tissues, with *STAT1*, *CCL5*, CXCL10, and *ITGB2* being significantly upregulated. However, *CCL2* expression is slightly higher in normal breast tissues (Figure 5). No variation in *GBP1* gene expression is observed between normal and tumor breast tissues. Furthermore, the gene expression of most of the PLR regulatory network genes is upregulated in metastatic breast tissues compared to normal breast tissues (Figure 5). Nonetheless, *PDCD1* gene expression is downregulated in metastatic breast tissues compared to normal breast tissues. This analysis is conducted using TNMplot.

The expression pattern of *PDCD1-PLR* genes in *HER2+* breast cancer tissues compared to normal, luminal breast cancer, and triple negative breast cancer (TNBC) tissues was examined via UALCAN (Supplementary Figure 1). The expression pattern of *PDCD1-PLR* genes is similar to *GEPIA*; 9 genes are upregulated in *HER2+* compared to normal breast tissues. B2M shows no statistically significant difference. 10 genes are highly upregulated in TNBC compared to normal and other subtypes. The *PDCD1-PLR* gene expression in *HER2*⁺ and *HER2–* breast cancer samples was analyzed using bc-GenExMiner v5.2 (Supplementary Figure 2). The findings point out that all genes are upregulated significantly in *HER2*⁺ compared to *HER2–* breast cancer.

Eventually, the association between *PDCD1-PLR* gene expression and *TP53* mutation status was assessed in breast cancer via UALCAN (Supplementary Figure 3). *TP53* is a crucial tumor suppressor gene frequently mutated in breast cancer. This analysis illustrated that the group with the *TP53* mutation had significantly higher expression levels of the *PDCD1-PLR* gene compared to the unmutated group. Gene expression data of lapatinib-resistant *HER2*⁺,

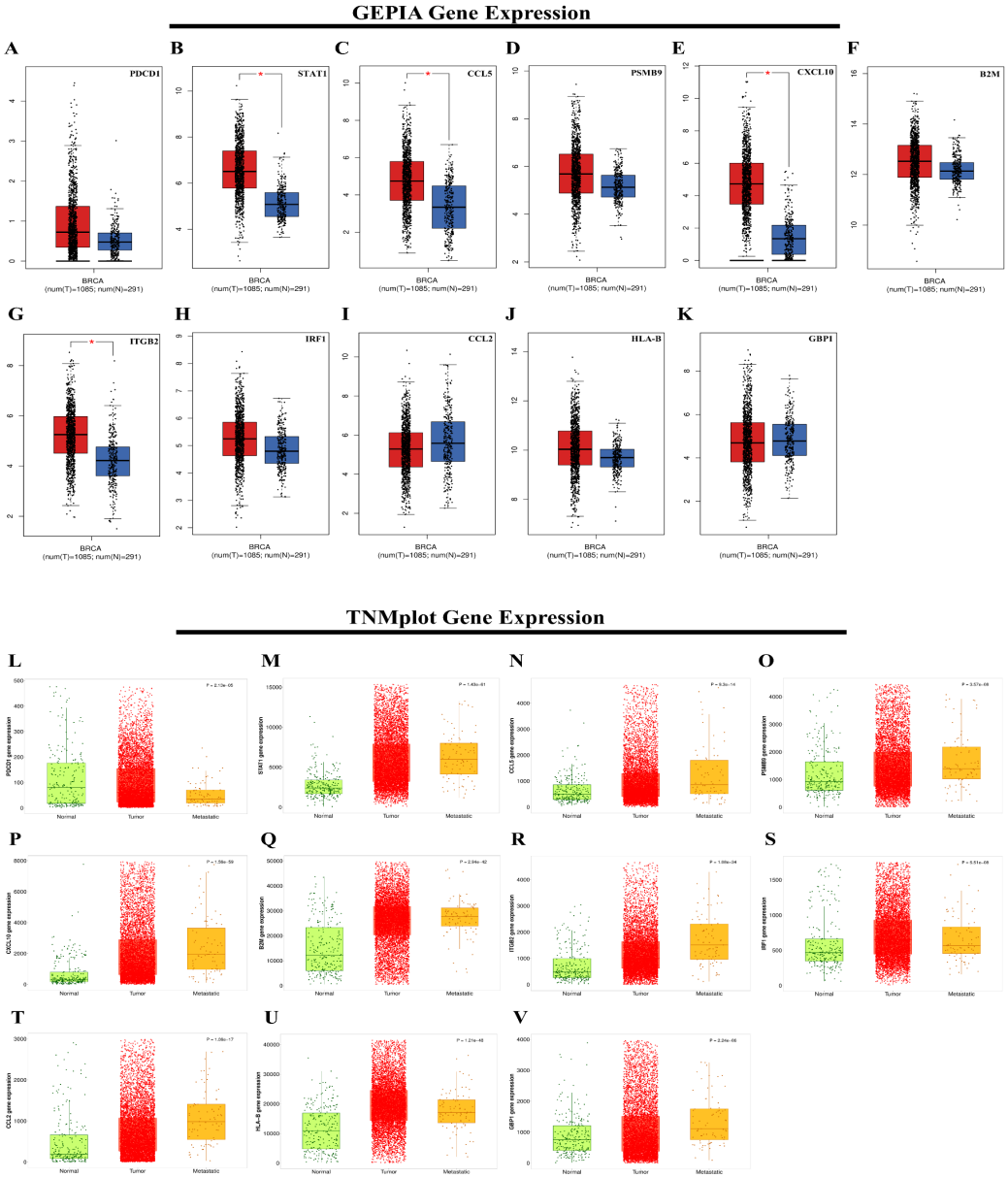

Figure 5. Gene expression of *PDCD1* and *PLR-hub* genes in normal breast tissues, tumor breast tissues, and metastatic breast tissues. GEPIA gene expression of *PDCD1* and *PLR-hub* genes in normal breast tissues and tumor breast tissues, analyzed by a modified version of the Student's t-test. (A) *PDCD1* gene expression. (B) *STAT1* gene expression. (C) *CCL5* gene expression. (D) *PSMB9* gene expression. (E) CXCL10 gene expression. (F) *B2M* gene expression. (G) *ITGB2* gene expression. (H) IRF1 gene expression. (I) *CCL2* gene expression. (J) *HLA-B* gene expression. (K) *GBP1* gene expression. TNMplot gene expression of *PDCD1* and *PLR-hub* genes in normal breast tissues, tumor breast tissues, and metastatic breast tissues, analyzed by Kruskal-Wallis Test. (L) *PDCD1* gene expression. (M) *STAT1* gene expression. (N) *CCL5* gene expression. (O) *PSMB9* gene expression. (P) *CXCL10* gene expression. (Q) B2M gene expression. (R) *ITGB2* gene expression. (S) *IRF1* gene expression. (T) *CCL2* gene expression. (U) *HLA-B* gene expression. (V) *GBP1* gene expression.

derived from SKBR3 cells with mutant-*TP53*, shows that *PDCD1*, *ITGB2*, and B2M gene expression remains upregulated. These findings hypothesize a potential link between *TP53* mutation and the upregulation of *PDCD1*, *ITGB2*, and B2M genes, highlighting the crosstalk between mutant-*TP53* and the elevation of these genes in lapatinib-resistant *HER2*$^{+}$ breast cancer.

Correlation between the gene expression of PDCD1 and PLR-hub genes

The correlation analyses between *PDCD1* and the *PLR* gene regulatory network in *HER2*+ breast cancer cells are conducted via *GEPIA* and TIMER 2.0 (Supplementary Figure 4A and 4B). The outcomes between the two tools are similar, validating the readouts. All PLR genes are significantly positively correlated. *CCL5*, *PSMB9, CXCL10, ITGB2,* and *IRF1* strongly correlated with *PDCD1*. Furthermore, *STAT1* and B2M are moderately correlated. *HLA-B* and *GBP1* genes fluctuate between moderate and strong correlation in *GEPIA* and TIMER 2.0. Nevertheless, *CCL2* is moderately correlated in TIMER 2.0 and weakly correlated in *GEPIA*. The positive

Table 3. Mutual Exclusivity Analysis of the PLR Regulatory Network

Gene A	Gene B	Log2 Odds Ratio	p-value	q-value	Tendency
PSMB9	*HLA-B*	>3	<0.001	<0.001	Co-occurrence
CCL5	*CCL2*	>3	<0.001	<0.001	Co-occurrence
PSMB9	*GBP1*	>3	0.017	0.263	Co-occurrence
HLA-B	*GBP1*	>3	0.023	0.263	Co-occurrence
ITGB2	*HLA-B*	2.886	0.041	0.416	Co-occurrence

correlation suggests potential co-regulation, shared pathway involvement, or common microenvironmental influences.

Survival analysis

Survival analysis of the PLR gene regulatory network in *HER2*$^+$/ER–/PR– breast cancer patients was conducted via KMPlotter depending on the prognostic value. The findings demonstrate that patients with elevated mRNA of *STAT1*, *PSMB9*, *CXCL10, B2M, HLA-B*, and *GBP1* have better RFS than patients with reduced mRNA levels (Supplementary Figure 4C). However, in the *HER2*$^+$/ER–/PR– lapatinib resistance gene expression data, *STAT1*, *PSMB9*, CXCL10, *HLA-B*, and *GBP1* are downregulated, which worsens the RFS. B2M is upregulated in the lapatinib resistance group; however, its upregulation alone does not correlate with improved survival outcomes. *PDCD1* alone does not stratify survival here (HR ≈1.08 (0.58 - 2.02), p = 0.81). That may reflect the complexity of *PD-1* biology, as elevated *PD-1* can show either active anti-tumor immunity or terminal exhaustion; thereby, it is not a straightforward prognostic marker.

Genetic alteration analysis of PDCD1 and PLR-hub genes

The genetic alteration analysis is performed for *PDCD1-PLR-hub* genes in breast cancer samples using the cBioportal, depending on the TCGA PanCancer atlas study. The oncoprint analysis of genetic alteration frequency in *PDCD1-PLR* genes shows that the percentage of alterations in breast cancer samples occurred in 0.7% to 2.3%, and most alterations are amplifications and deep deletions (Supplementary Figure 5). Moreover, the copy number alterations versus gene expression for *PDCD1-PLR-hub* genes are presented. A monotonic dosage effect is observed; breast tumors with fewer copies (deep/shallow deletions) have lower *PDCD1-PLR* expression, breast tumors with normal copies (diploid) sit at a baseline, and breast tumors with more copies (gains/amplifications) have higher *PDCD1-PLR* expression. These genomic alterations in breast tumors could up- or down regulate *PDCD1-PLR* gene expression, potentially reinforcing either an immune active or an immune cold state. Further mutual exclusivity analysis exhibited that five significant gene pairs co-occurred in mutation, *PSMB9-HLA-B*, *CCL5-CCL2*, *PSMB9- GBP1*, *HLA-B- GBP1*, and *ITGB2-HLA-B* (Table 3).

Discussion

The evolution of lapatinib resistance in *HER2*$^+$/ER–/PR– breast cancer exemplifies the complex crosstalk between tumor-intrinsic oncogenic signaling rewiring and immune microenvironmental reprogramming [1]. This study determined the tumor-intrinsic *PD-1*-centered regulatory network (*PDCD1-PLR* regulatory network) that drives immunosuppressive microenvironment adaptation, permitting immune evasion and aggressive breast tumor behavior. Through diverse bioinformatics analyses, a mechanistic model was defined where lapatinib resistance is orchestrated not only by *HER2*$^+$ pathway restoration but also by substantial immunomodulatory reprogramming (Supplementary Figure 6). These observations harmonize with evolving evidence that targeted therapies unexpectedly trigger the TME to favor resistance via cancer immunoediting mechanisms, a phenomenon that is progressively recognized in *HER2*+ breast tumors [13,14].

PD-1 is a checkpoint receptor that represses T cell effector functions via SHP-2-mediated dephosphorylation of TCR signaling components [5]. Gene expression findings of lapatinib resistance *HER2*$^+$/ER–/PR– breast cancer indicate that the center of the network, tumor-intrinsic *PDCD1* (*PD-1*), is upregulated. While *PD-1* inhibitors have revolutionized cancer immunotherapy, the insights uncover *HER2* a paradoxical impact of tumor-intrinsic *PD-1* in *HER2*+ resistance, which has received much less attention than the typical *PD-1* expressed on immune cells. Recent findings demonstrate that tumor-intrinsic *PD-1* triggers carcinogenesis in melanoma, hepatocellular carcinoma, pancreatic ductal adenocarcinoma, thyroid cancer, glioblastoma, and TNBC [9,15,16]. Thus, breast tumor cells can express *PD-1* and engage ligand interactions in cis or trans, such as *PD-L1* and *PD-L2*, to stimulate oncogenic intracellular signaling, promoting progression and survival independent of adaptive immunity. *PD-1*/*PD-L1* interactions within breast tumor cells have been shown to induce chemoresistance via activation of the PI3K/Akt, MAPK/ERK, and mTOR pathways and upregulation of drug-efflux pumps [9,17]. A previous study has shown that Y-box binding protein 1 (YB-1) is aberrantly upregulated in TNBC and promotes tumor-intrinsic *PD-1*/*PD-L1* expression via translational stimulation, leading to TNBC progression. However, silencing YB-1 can inhibit tumorigenesis and metastatic potential, but these inhibitory effects are completely rescued by exogenous *PD-1*/*PD-L1* expression [18].

In the tumor-intrinsic *PDCD1-PLR* regulatory network, IFN-responsive genes (*STAT1, IRF1, CXCL10, CCL5*) and antigen presentation machinery genes (*PSMB9*, *HLA-B*) are suppressed in lapatinib-resistant groups, generating a cold TME, distinguished by impaired T cell recruitment and deregulated antigen processing.

Preclinical data in murine *HER2*$^+$ models demonstrate that lapatinib can enhance *STAT1*-dependent anti-tumor immunity by increasing IFNγ-secreting CD8$^+$ T cells and chemokines such as *CXCL10* [19]. The data state that *STAT1* deficiency in lapatinib-resistant cells abrogates this effect and impairs T cell infiltration, proposing a tumor-intrinsic rewiring that silences IFNγ signaling and chemokine biosynthesis to evade immune surveillance. *IRF1*, a central regulator of IFNγ-induced gene expression and pro-apoptotic signaling, is similarly inhibited in lapatinib-resistant *HER2*+ cells, shifting breast tumors towards progression and hindering the normal activation of antigen-processing genes and immunogenic cell death pathways [20]. The lower level of *STAT1* and *IRF1* suggests an adaptive resistance mechanism for immune escape.

On the other hand, a paradoxical upregulation of B2M and *ITGB2* gene expression is observed in lapatinib-resistant cells, which reflects a dual role, preserving MHC-I complexes to prolong chronic antigen presentation, resulting in T cell exhaustion, while promoting leukocyte cell adhesion through *ITGB2*, driving the infiltration of M0 and M2 macrophages, MDSCs, and Tregs. Integrins also explain moderately infiltrated monocytes and neutrophils. B2M elevation may also show dysregulated MHC I turnover associated with immune escape. MDSCs secrete IL-10 and TGF-β to attenuate T cell responses, while CAFs generate extracellular matrix proteins that obstruct breast tumors from immune cell infiltration. Therefore, lapatinib-resistant breast cancer cells may depend on a feedback loop by hijacking *PD-1* signaling to stimulate stromal barriers while repressing chemokine-driven immune stimulation [21–23]. This is consistent with the outcomes of the study, illustrating that *ITGB2* elevation in breast cancer may stimulate metastasis via immune-suppressive stromal interactions.

The immune infiltration analysis illustrates that most of the tumor-intrinsic PLR genes are positively correlated with anti-tumor immune cell infiltration in *HER2*+, highlighting the baseline immunogenicity of *HER2*+ breast cancer; thus, if these PLR genes are inhibited, this could lead to an overall decrease in anti-tumor immune cell infiltration and may also result in cold immunosuppressive TME by elevating MDSCs, Tregs, and CAFs, making breast cancer cells less responsive to targeted treatments and immunotherapy [13,24,25]. Interestingly, in the lapatinib-resistant groups, *PDCD1*, *ITGB2*, and B2M remained upregulated while other PLR genes (*STAT1, CCL5, PSMB9, CXCL10, IRF1, CCL2, HLA-B*, and *GBP1*) were reduced. *PD-1*/*PD-L1* axis in lapatinib-resistant breast tumors/CD8+ T cells transfers potent inhibitory signals via SHP2-mediated dephosphorylation of TCR signaling intermediates, exhausting T cells, and attenuating anti-tumor immune responses [26]. Previous studies discussed that *CXCL10* is a central chemoattractant for CXCR3+ cytotoxic T cells and NK cells, and its loss has been associated with immune exclusion in melanoma and colorectal cancer. Furthermore, *CCL5* recruits CCR5+ dendritic cells and T cells, and its inhibition in resistant cancer cells results in a myeloid dendritic cell quiescent state [27–29]. Despite elevated dendritic cells in lapatinib-resistant samples, *STAT1*/*IRF1* and *CXCL10/CCL5* are repressed, implying possible impaired function or inefficient antigen presentation, resulting in immune evasion. The elevated infiltrated dendritic cells could be exploited via an ex vivo-generated dendritic cell-based vaccine loaded with tumor antigens to enhance antitumor immunity [30]. Furthermore, the broad suppression of interferon signaling, chemokine-mediated immune recruitment, and the persistent *PD-1* expression may reflect dysfunctional or ineffective T cell responses, potentially contributing to immune evasion and therapeutic resistance. These data indicate that immune exhaustion is a key characteristic of lapatinib resistance and suggest that *PD-1* inhibition or IFN pathway reactivation may help reverse the immunosuppressive state, enhance T-cell infiltration, and overcome resistance [31].

Gene ontology analysis supports the immune involvement, and KEGG pathway analysis strengthens this model, revealing immune-metabolic interplay as a resistance driver. Clusters 1-3, viral infection and cytokine signaling pathways, highlight the tumor's mimicry of chronic inflammatory states that lead to persistent antigen exposure and thus T cell exhaustion. This oncogenic mechanism is recognized in hepatitis B-associated hepatocellular carcinoma. On the other hand, clusters 4-5, metabolic and hormonal signaling, indicate lipid metabolism rewiring involvement in lapatinib resistance *HER2*+ breast cancer cells. The gene-metabolites analysis also validated these results, indicating that the PLR regulatory network is involved in lipid metabolic reprogramming and oncogenic signaling. Thus, resistant *HER2*+ breast tumors shift metabolism to synthesize cholesterol that stimulates PI3K/AKT signaling, an axis implicated in *HER2*+ breast cancer resistance, while nurturing an immunosuppressive lipid raft environment that sequesters TCR signaling components [32]. The data also demonstrate potential immune evasion via the androgen receptor signaling, disrupting normal MHC-I expression and promoting T cell exclusion [33].

Survival and genetic alteration analyses present a translational relevance of the PLR regulatory network findings. The correlation between the elevated expression of *STAT1*, *PSMB9*, and *HLA-B* and the enhanced prognosis in *HER2*$^+$/ER–/PR– breast cancer aligns with their roles in antigen presentation and IFNγ responsiveness. However, these genes are downregulated in lapatinib-resistant cells, and the elevated B2M represents the duality of immune biomarkers, due to its role in antigen presentation and T cell exhaustion. On the other hand, genetic alteration analysis explains that genomic instability is not the primary resistance driver. Comparative gene expression profiling demonstrates that most *PLR-hub* genes are overexpressed in baseline breast tumors compared to normal breast tissue, with the highest expression in metastatic and *TP53* mutant backgrounds; however, in lapatinib-resistant cells, the expression pattern differs. The focal copy number gains/amplifications in *PDCD1*, *ITGB2*, and B2M can generate high gene expression in a small subset of breast tumors; however, such gains/amplifications occur in fewer than 2% of breast cancer cases and cannot elucidate the uniform upregulation

of these genes observed in lapatinib resistant breast cancer cells, implicating lapatinib induced epigenetic or transcriptional modulations instead of genomic alteration alone [34,35]. The low frequency of *PDCD1* alterations (1.2%) further implicates transcriptional regulation via NFATc1 or AP-1, factors stimulated by *HER2*/EGFR signaling. Moreover, the consistent downregulation of IFN-responsive and antigen presentation genes (*STAT1*, *CCL5*, *PSMB9*, *CXCL10, IRF1, CCL2, HLA-B,* and *GBP1*) indicates widespread suppression of IFNγ signaling and chemokine expression beyond copy number alterations.

These findings recommend several therapeutic approaches to tackle lapatinib resistance in breast cancer by addressing both tumor-intrinsic signaling and extrinsic immune dysfunction. Combining *PD-1* inhibitors with agents that restore IFNγ signaling, such as stimulator of interferon genes (STING) agonists, or intratumoral IFNγ that could reverse chemokine inhibition and restore MHC-I normal function. Previous experiments on TNBC show that STING agonists synergize with anti-*PD-1* therapy to promote CD8+ T cell infiltration and dendritic cell maturation [31]. A prior study exhibited that lapatinib combination with the TLR7 agonist SZU-101 maintains immunostimulatory activity and promotes tumor clearance, making it a promising candidate for combined immunotherapy/targeted therapy. Other tyrosine kinase inhibitors, such as sunitinib, dasatinib, and sorafenib may interfere with immune activation and should be selected with caution in such combination protocols [36]. The data hypothesize that epigenetic modifiers, including DNA methyltransferase or histone deacetylase inhibitors (HDAC) inhibitors, could restore *STAT1* and *CCL5* expression. Further evidence has illustrated that promoting immunoproteasome function through cytokine therapy or small molecule agonists could raise *PSMB9* expression and enhance proteasome function, resulting in better survival in several cancer types [37]. Metabolic interventions targeting lipid synthesis, such as fatty acid synthase (FASN) inhibitors, or cholesterol trafficking, such as statins, can also disrupt immunosuppressive signaling. Statins also enhance innate immunity in breast cancer by suppressing mutant-*TP53* [38,39]. A prior study has demonstrated that high membrane cholesterol preserves *HER2*+ at the cell surface by elevating membrane rigidity. Thus, decreasing cholesterol via lovastatin enhances internalization and degradation of *HER2*+, which promotes the efficacy of lapatinib. Experiments on mouse models have shown that combining lovastatin with lapatinib significantly mitigated breast tumor growth [40]. A prior experiment showed that combining MRTX849 with lapatinib significantly enhanced treatment efficacy in mice having KRASG12C-mutant head and neck cancer. Immune analysis exhibited upregulation of *PD-L1* and changes in TME composition, including $CD8^+$ T cell dynamics. However, depletion of $CD8^+$ T cells decreased therapy effectiveness, while adding anti-*PD-1* (α*PD-1*) therapy improved anti-tumor responses, especially in resistant tumors. These findings suggest that targeting bypass pathways and modulating the immune microenvironment are essential approaches to tackle resistant KRASG12C-mutant head and neck cancer [41]. These observations are promising and recommend applying this protocol to tackle lapatinib resistance in *HER2*+ breast cancer.

PANACEA phase 1b-2 trial has demonstrated that the combination of pembrolizumab (a *PD-1* inhibitor) and trastuzumab in patients with advanced, *HER2*+ trastuzumab-resistant breast cancer is safe and potentially beneficial in *PD-L1*-positive cases, highlighting the role of immune mechanisms in resistance. Another approach is adoptive cell therapies, such as engineered chimeric antigen receptor (CAR) T cells or tumor-infiltrating lymphocyte infusions, that reversed exhausted T cells via blocking *PD-1* and promoting chemokine-mediated trafficking. Previous evidence exhibits that third-generation anti-*HER2* CAR-T cells effectively target trastuzumab-resistant *HER2*+ breast cancer cells in vitro and in vivo. Therefore, combining CAR-T cells with *PD-1* blockade further improved their cytotoxicity and tumor inhibition, showing a potential approach to tackle *HER2*+ breast cancer resistance [42]. These approaches and studies present insights into the mechanisms of lapatinib resistance. Comprehending these approaches is significant for the development of effective strategies to tackle lapatinib resistance and enhance patient outcomes.

In conclusion, this integrative bioinformatic and transcriptomic analyses identify the tumor-intrinsic PLR regulatory network implicated in lapatinib resistance through dynamically reprogramming the *HER2*$^+$/ER–/PR– breast cancer TME. Lapatinib-resistant breast cancer cells can evade the immune system via multiple mechanisms, including amplifying immunosuppressive signals, silencing interferon responses, and impairing efficient antigen presentation. These insights argue for a paradigm shift in *HER2*+ breast cancer targeted therapy by introducing combinatorial regimens that co-target immune and metabolic pathways implicated in resistance. This study was based on computational analyses of GEO data. The relatively small sample size may affect statistical power, and gene expression changes do not always correspond to protein-level alterations due to post-transcriptional regulation. Experimental validation will be required to confirm and extend these outcomes. Future research should focus on validating the tumor-intrinsic PLR regulatory network in patient-derived organoids to map stromal-immune interactions in resistant niches and revolutionize personalized immuno-oncology approaches for *HER2*+ breast cancer.

Author Contribution Statement

All authors contributed equally in this study.

Acknowledgements

Ethical Approval

This study is an integrative bioinformatics analysis and does not need ethical approval.

Data Availability

The GSE38376 dataset downloaded and analyzed

during the current study is available in the Gene Expression Omnibus (GEO) repository and can be directly accessed using (https://www.ncbi.nlm.nih.gov/geo/query/acc.cgi?acc=GSE38376). Other data generated or analyzed during this study are included in the article and supplementary material files.

References

1. Wahdan-Alaswad R, Liu B, Thor AD. Targeted lapatinib anti-*HER2*/erbb2 therapy resistance in breast cancer: Opportunities to overcome a difficult problem. Cancer Drug Resist. 2020;3(2):179-98. https://doi.org/10.20517/cdr.2019.92.
2. Lin CH, Pelissier FA, Zhang H, Lakins J, Weaver VM, Park C, et al. Microenvironment rigidity modulates responses to the *HER2* receptor tyrosine kinase inhibitor lapatinib via yap and taz transcription factors. Mol Biol Cell. 2015;26(22):3946-53. https://doi.org/10.1091/mbc.E15-07-0456.
3. Sharpe AH, Pauken KE. The diverse functions of the pd1 inhibitory pathway. Nat Rev Immunol. 2018;18(3):153-67. https://doi.org/10.1038/nri.2017.108.
4. Dong P, Xiong Y, Yue J, Hanley SJB, Watari H. Tumor-intrinsic *PD-L1* signaling in cancer initiation, development and treatment: Beyond immune evasion. Front Oncol. 2018;8:386. https://doi.org/10.3389/fonc.2018.00386.
5. Lin X, Kang K, Chen P, Zeng Z, Li G, Xiong W, et al. Regulatory mechanisms of *PD-1*/*PD-L1* in cancers. Mol Cancer. 2024;23(1):108. https://doi.org/10.1186/s12943-024-02023-w.
6. Alhallaq AS, Sultan NS. Decoding nf-κb: Nucleocytoplasmic shuttling dynamics, synthetic modulation and post-therapeutic behavior in cancer. Mol Biol Rep. 2025;52(1):804. https://doi.org/10.1007/s11033-025-10917-1.
7. Hermawan A, Putri H. Bioinformatics analysis of programmed death-1-trastuzumab resistance regulatory networks in breast cancer cells. Asian Pac J Cancer Prev. 2025;26(1):279-92. https://doi.org/10.31557/apjcp.2025.26.1.279.
8. Triulzi T, Forte L, Regondi V, Di Modica M, Ghirelli C, Carcangiu ML, et al. *HER2* signaling regulates the tumor immune microenvironment and trastuzumab efficacy. Oncoimmunology. 2019;8(1):e1512942. https://doi.org/10.1080/2162402x.2018.1512942.
9. Chen M, Bie L, Ying J. Cancer cell-intrinsic *PD-1*: Its role in malignant progression and immunotherapy. Biomed Pharmacother. 2023;167:115514. https://doi.org/10.1016/j.biopha.2023.115514.
10. Suh KJ, Sung JH, Kim JW, Han SH, Lee HS, Min A, et al. Egfr or *HER2* inhibition modulates the tumor microenvironment by suppression of *PD-L1* and cytokines release. Oncotarget. 2017;8(38):63901-10. https://doi.org/10.18632/oncotarget.19194.
11. Komurov K, Tseng JT, Muller M, Seviour EG, Moss TJ, Yang L, et al. The glucose-deprivation network counteracts lapatinib-induced toxicity in resistant erbb2-positive breast cancer cells. Mol Syst Biol. 2012;8:596. https://doi.org/10.1038/msb.2012.25.
12. Steen CB, Liu CL, Alizadeh AA, Newman AM. Profiling cell type abundance and expression in bulk tissues with cibersortx. Methods Mol Biol. 2020;2117:135-57. https://doi.org/10.1007/978-1-0716-0301-7_7.
13. Batalha S, Gomes CM, Brito C. Immune microenvironment dynamics of *HER2* overexpressing breast cancer under dual anti-*HER2* blockade. Front Immunol. 2023;14:1267621. https://doi.org/10.3389/fimmu.2023.1267621.
14. Hanna A, Balko JM. Breast cancer resistance mechanisms: Challenges to immunotherapy. Breast Cancer Res Treat. 2021;190(1):5-17. https://doi.org/10.1007/s10549-021-06337-x.
15. Martins C, Rasbach E, Heppt MV, Singh P, Kulcsar Z, Holzgruber J, et al. Tumor cell-intrinsic *PD-1* promotes merkel cell carcinoma growth by activating downstream mtor-mitochondrial ros signaling. Sci Adv. 2024;10(3):eadi2012. https://doi.org/10.1126/sciadv.adi2012.
16. Yao H, Wang H, Li C, Fang JY, Xu J. Cancer cell-intrinsic *PD-1* and implications in combinatorial immunotherapy. Front Immunol. 2018;9:1774. https://doi.org/10.3389/fimmu.2018.01774.
17. Black M, Barsoum IB, Truesdell P, Cotechini T, Macdonald-Goodfellow SK, Petroff M, et al. Activation of the *PD-1*/*PD-L1* immune checkpoint confers tumor cell chemoresistance associated with increased metastasis. Oncotarget. 2016;7(9):10557-67. https://doi.org/10.18632/oncotarget.7235.
18. Wu Q, Xu Y, Li X, Liu H, You T, Cai T, et al. Yb-1 promotes cell proliferation and metastasis by targeting cell-intrinsic *PD-1*/*PD-L1* pathway in breast cancer. Int J Biochem Cell Biol. 2022;153:106314. https://doi.org/10.1016/j.biocel.2022.106314.
19. Hannesdóttir L, Tymoszuk P, Parajuli N, Wasmer MH, Philipp S, Daschil N, et al. Lapatinib and doxorubicin enhance the *STAT1*-dependent antitumor immune response. Eur J Immunol. 2013;43(10):2718-29. https://doi.org/10.1002/eji.201242505.
20. Schwartz JL, Shajahan AN, Clarke R. The role of interferon regulatory factor-1 (*IRF1*) in overcoming antiestrogen resistance in the treatment of breast cancer. Int J Breast Cancer. 2011;2011(1):912102. https://doi.org/https://doi.org/10.4061/2011/912102.
21. Zu L, He J, Zhou N, Zeng J, Zhu Y, Tang Q, et al. The profile and clinical significance of *ITGB2* expression in non-small-cell lung cancer. J Clin Med. 2022;11(21):6421. https://doi.org/10.3390/jcm11216421.
22. Zhang H, Cui B, Zhou Y, Wang X, Wu W, Wang Z, et al. B2m overexpression correlates with malignancy and immune signatures in human gliomas. Sci Rep. 2021;11(1):5045. https://doi.org/10.1038/s41598-021-84465-6.
23. Fan J, Sha T, Ma B. Cancer-derived extracellular vesicle *ITGB2* promotes the progression of triple-negative breast cancer via the activation of cancer-associated fibroblasts. Global Challenges. 2025;9(3):2400235. https://doi.org/https://doi.org/10.1002/gch2.202400235.
24. Watson SS, Dane M, Chin K, Tatarova Z, Liu M, Liby T, et al. Microenvironment-mediated mechanisms of resistance to *HER2* inhibitors differ between *HER2*+ breast cancer subtypes. Cell Syst. 2018;6(3):329-42.e6. https://doi.org/10.1016/j.cels.2018.02.001.
25. Zhang X, Dong Y, Zhao M, Ding L, Yang X, Jing Y, et al. Itgb2-mediated metabolic switch in cafs promotes oscc proliferation by oxidation of nadh in mitochondrial oxidative phosphorylation system. Theranostics. 2020;10(26):12044-59. https://doi.org/10.7150/thno.47901.
26. Wu X, Yang H, Yu X, Qin JJ. Drug-resistant *HER2*-positive breast cancer: Molecular mechanisms and overcoming strategies. Front Pharmacol. 2022;13:1012552. https://doi.org/10.3389/fphar.2022.1012552.
27. De Angelis C, Nagi C, Hoyt CC, Liu L, Roman K, Wang C, et al. Evaluation of the predictive role of tumor immune infiltrate in patients with *HER2*-positive breast cancer treated with neoadjuvant anti-*HER2* therapy without

chemotherapy. Clin Cancer Res. 2020;26(3):738-45. https://doi.org/10.1158/1078-0432.Ccr-19-1402.
28. Groom JR, Luster AD. Cxcr3 in t cell function. Exp Cell Res. 2011;317(5):620-31. https://doi.org/10.1016/j.yexcr.2010.12.017.
29. Rawat K, Tewari A, Li X, Mara AB, King WT, Gibbings SL, et al. Ccl5-producing migratory dendritic cells guide ccr5+ monocytes into the draining lymph nodes. J Exp Med. 2023;220(6). https://doi.org/10.1084/jem.20222129.
30. Lee KW, Yam JWP, Mao X. Dendritic cell vaccines: A shift from conventional approach to new generations. Cells. 2023;12(17). https://doi.org/10.3390/cells12172147.
31. Razaghi A, Durand-Dubief M, Brusselaers N, Björnstedt M. Combining *PD-1*/*PD-L1* blockade with type i interferon in cancer therapy. Front Immunol. 2023;14:1249330. https://doi.org/10.3389/fimmu.2023.1249330.
32. Feng WW, Kurokawa M. Lipid metabolic reprogramming as an emerging mechanism of resistance to kinase inhibitors in breast cancer. Cancer Drug Resist. 2020;3(1):1-17. https://doi.org/10.20517/cdr.2019.100.
33. Chesner LN, Polesso F, Graff JN, Hawley JE, Smith AK, Lundberg A, et al. Androgen receptor inhibition increases mhc class i expression and improves immune response in prostate cancer. Cancer Discov. 2025;15(3):481-94. https://doi.org/10.1158/2159-8290.Cd-24-0559.
34. Nami B, Ghanaeian A, Black C, Wang Z. Epigenetic silencing of *HER2* expression during epithelial-mesenchymal transition leads to trastuzumab resistance in breast cancer. Life (Basel). 2021;11(9):868. https://doi.org/10.3390/life11090868.
35. Lee J, Bartholomeusz C, Mansour O, Humphries J, Hortobagyi GN, Ordentlich P, et al. A class i histone deacetylase inhibitor, entinostat, enhances lapatinib efficacy in *HER2*-overexpressing breast cancer cells through foxo3-mediated bim1 expression. Breast Cancer Res Treat. 2014;146(2):259-72. https://doi.org/10.1007/s10549-014-3014-7.
36. Gao N, Zhong J, Wang X, Jin Z, Li W, Liu Y, et al. Immunomodulatory and antitumor effects of a novel tlr7 agonist combined with lapatinib. Sci Rep. 2016;6:39598. https://doi.org/10.1038/srep39598.
37. Chen B, Zhu H, Yang B, Cao J. The dichotomous role of immunoproteasome in cancer: Friend or foe? Acta Pharmaceutica Sinica B. 2023;13(5):1976-89. https://doi.org/https://doi.org/10.1016/j.apsb.2022.11.005.
38. Wang Z, Shi M, Liu B, Zhang X, Lin W, Yang Y, et al. Low-dose statins restore innate immune response in breast cancer cells via suppression of mutant p53. Front Pharmacol. 2025;16:1492305. https://doi.org/10.3389/fphar.2025.1492305.
39. Cuyàs E, Pedarra S, Verdura S, Pardo MA, Espin Garcia R, Serrano-Hervás E, et al. Fatty acid synthase (fasn) is a tumor-cell-intrinsic metabolic checkpoint restricting t-cell immunity. Cell Death Discov. 2024;10(1):417. https://doi.org/10.1038/s41420-024-02184-z.
40. Zhang J, Li Q, Wu Y, Wang D, Xu L, Zhang Y, et al. Cholesterol content in cell membrane maintains surface levels of erbb2 and confers a therapeutic vulnerability in erbb2-positive breast cancer. Cell Commun Signal. 2019;17(1):15. https://doi.org/10.1186/s12964-019-0328-4.
41. Novoplansky O, Jagadeeshan S, Prasad M, Yegodayev KM, Marripati D, Shareb RA, et al. Dual inhibition of hers and *PD-1* counteract resistance in kras(g12c)-mutant head and neck cancer. J Exp Clin Cancer Res. 2024;43(1):308. https://doi.org/10.1186/s13046-024-03227-0.
42. Li H, Yuan W, Bin S, Wu G, Li P, Liu M, et al. Overcome trastuzumab resistance of breast cancer using anti-*HER2* chimeric antigen receptor t cells and pd1 blockade. Am J Cancer Res. 2020;10(2):688-703.